



**Kinematic Behaviour of a Novel Pedicle Screw-Rod Fixation System for the Canine Lumbosacral Joint**

Journal:	<i>Veterinary Surgery</i>
Manuscript ID	VSU-16-053.R5
Manuscript Type:	Original Article - Research
Keywords:	4-point bending, biomechanical testing, orthopedic biomechanics, orthopedic implant, spinal surgery

SCHOLARONE™  
Manuscripts

Review

1 **ABSTRACT**

2 **Objective:** To determine the biomechanical behaviour of a novel distraction-  
3 stabilization system, consisting of an intervertebral distraction bolt, polyaxial screws  
4 and connecting rods, in the canine lumbosacral spine.

5 **Study design:** Biomechanical study.

6 **Sample population:** Cadaveric canine lumbosacral spines (L4-Cd3) (N=8)

7 **Methods:** Cadaveric lumbosacral spines were harvested, stripped of musculature,  
8 mounted on a 4-point bending jig, and tested in extension, flexion and lateral bending  
9 using non-destructive compressive axial loads (0-150N). Angular displacement was  
10 recorded from reflective optical trackers rigidly secured to L6, L7 and S1. Data for  
11 primary and coupled motion were collected from intact spines; after destabilization at  
12 L7-S1, and following surgical stabilisation with the new implant system.

13 **Results:** As compared with the intact spine, laminectomy resulted in a modest  
14 increase in angular displacement at L6-L7 and a marked increase at L7-S1.  
15 Instrumentation significantly reduced motion at the operated level (L7-S1) with a  
16 concomitant increase at the adjacent level (L6-L7).

17 **Conclusion:** The combination of a polyaxial pedicle screw-rod system and  
18 intervertebral spacer provides a versatile solution of surgical stabilisation of the  
19 lumbosacral joint following surgical decompression in the canine lumbosacral spine.  
20 The increase in motion at L6-L7 may suggest the potential for adjacent level effects  
21 and clinical trials should be designed to address this question.

22 **Clinical relevance:** These results support the feasibility of using this new implant  
23 system for the management of degenerative lumbosacral disease in dogs. The increase  
24 in motion at L6-L7 may suggest the potential for adjacent level effects and clinical  
25 trials should be designed to address this question.

26

## 27 INTRODUCTION

28 Surgical treatment of degenerative lumbosacral disease has been recommended for  
29 dogs with severe pain.<sup>1</sup> Decompressive surgery is considered an appropriate technique  
30 to relieve compression of the cauda equina and nerve roots in dogs with degenerative  
31 lumbosacral stenosis (DLSS)<sup>2</sup>, and dorsal laminectomy with or without annulectomy  
32 and partial discectomy is currently the most commonly performed surgery.<sup>3-6</sup> Clinical  
33 results with this technique have shown to have overall success rates between 79% and  
34 93.2%.<sup>4,7</sup> But recent studies have reported deterioration several weeks  
35 postoperatively<sup>5</sup> with inferior force plate parameters 6 months postoperatively  
36 compared to normal dogs.<sup>8</sup>

37  
38 Several lumbosacral fixation techniques have been evaluated in dogs, with variable  
39 results.<sup>3,9,10-15</sup> Trans-articular facet screw fixation has been plagued with a high  
40 incidence of technical failure without effective stabilisation.<sup>16</sup> Pedicle screw fixation  
41 systems are widely used in human medicine and it has been shown that paired pedicle  
42 screws inserted in lumbar vertebrae at 30° offered more resistance to axial pull-out  
43 than paired pedicle screws placed parallel.<sup>17</sup> In a biomechanical study in canine spines  
44 the ideal pin insertion angle in the last lumbar vertebra was found to be 30°, providing  
45 the greatest amount of bone purchase with a wide margin of safety.<sup>18</sup> Biomechanical  
46 studies have shown that pedicle screw and rod fixation effectively stabilizes the  
47 lumbosacral spine in extension and flexion *in vitro*.<sup>19</sup> Clinically, pedicle screw-rod  
48 constructs applied after decompressive surgery have been associated with excellent  
49 stability, function and pain relief<sup>12</sup>, with increased propulsive forces on force plate  
50 analysis during a 6-month postoperative period, albeit without confirmation of  
51 successful fusion on histopathology.<sup>15,20</sup>

52 In a biomechanical study using a bovine calf spine model it was shown that stand-  
53 alone interbody fusion cages are effective in restoring neuroforaminal height and  
54 stabilize the spine to withstand foraminal deformation during daily loading<sup>21</sup>, which  
55 has been confirmed in humans to have optimal clinical outcomes preventing  
56 subsequent collapse of the intervertebral space and compression of cauda equina and  
57 nerve roots.<sup>22</sup> Interbody cage combined with pedicle screw fixation provided  
58 sufficient stability and stiffness in a finite element study<sup>23</sup> and met the criteria for  
59 lumbo-sacral fusion in a clinical study.<sup>24</sup>

60

61 We have recently developed a spinal implant system that consists of a threaded  
62 intervertebral bolt to distract the neuroforamina, and polyaxial pedicle-vertebral body  
63 screws with connecting rods to increase holding strength of the construct and promote  
64 interbody fusion. The objective of this cadaveric study was to determine the efficacy  
65 of the new fixation system in restoring stability to the lumbosacral spine after  
66 decompressive surgery. The hypotheses were that (1) the new instrumentation would  
67 lead to a significant reduction in primary and coupled motion at the operated L7-S1  
68 level after decompressive surgery and (2) that application of the new fixation system  
69 would not have a significant effect on the mobility of the adjacent L6-L7 disc space.

70

71

## 72 MATERIALS AND METHODS

### 73 *Specimens*

74 The pelvis and lumbar spine (L4 to the third caudal vertebra) were harvested *en bloc*  
75 from eight skeletally mature large dogs (median 29.7kg, range 25.0 to 39.5 kg) that  
76 were euthanized for reasons unrelated to this study. The specimens were collected  
77 under an approved Institutional Care and Use Committee (IACUC) protocol. Breeds  
78 represented were Pitbull (N=1), Rottweiler (N=2), Pitbull cross (N=3) and German  
79 Shepherd Dog (N=2). The age of the dogs was estimated by dentition to be 1-2 years  
80 (N=5) and 2-3 years old (N=3). Radiographs confirmed closure of the vertebral  
81 growth plates and ruled out pre-existing spinal pathology within the lumbar spine and  
82 L-S junction.

83

### 84 *Implants*

85 The instrumentation consists of a tapered intervertebral distraction bolt, polyaxial  
86 screws, clamps, connecting rods, washers and nuts (██████████  
87 ██████████) (Figs 1, 2), all machined from medical grade titanium alloy (Ti6Al4V).  
88 The intervertebral bolt (19mm long, tapering from a diameter of 7.5mm proximally to  
89 4.4mm distally) is coated with hydroxyapatite (HA) and has external positive profile  
90 threads (pitch of 2.125 mm and height of 1.49 mm above the surface of the spacer).  
91 The self-tapping cortical pedicle screws (4.5 mm, with a core diameter of 3.2mm) are  
92 available in lengths of 30, 35 and 40 mm. The rods with a diameter of 4mm have  
93 dumbbell ends, making it possible to lock the rods (between the washer and the nut)  
94 in any position within the polyaxial clamps. The rods, available in lengths of 32mm,  
95 37 mm and 42 mm, can be bent as needed to allow for placement around the articular  
96 facets of L7 and S1.

97

98 *Specimen preparation*

99 Muscle and soft tissue were removed from the specimens, taking care to leave  
100 ligamentous tissue (supraspinous ligament, interspinous ligament, capsules and  
101 ligaments of the articular facets) intact. The functional spinal units were disarticulated  
102 at the L4-L5 junction cranially and at the Cd3-Cd4 junction caudally, so that the final  
103 specimen included L5, L6, L7, the sacrum, the pelvis and Cd1-3. Immobilisation of  
104 L5-L6 and S3-Cd1 joints was achieved by placing wood screws bilaterally through  
105 the articulation between the adjacent vertebrae and perpendicular to the sacroiliac  
106 joints on each side. The accuracy of screw positioning was verified by radiography  
107 prior to testing (Fig 3). The cranial and caudal ends of the specimen, including the  
108 acetabulae, were embedded in 4" diameter PVC tubes filled with polyester resin  
109 (Bondo Body Filler; 3M, St Paul, MN) (Fig 3). After hardening, care was taken to  
110 ensure that the L6-L7 and L7-S1 articulations were freely mobile in flexion-extension  
111 and lateral bending. Specimens were wrapped in saline-soaked towels and frozen at  
112 -20C°. Before testing, the specimens were thawed for 24 hours at 4°C.

113

114 *Dorsal Laminectomy, Annulectomy and Discectomy.*

115 The supra- and interspinous ligaments were resected between L7 and S1 and the  
116 caudal one-quarter of the spinous process of L7 and the entire spinal process at S1-S2  
117 were removed with rongeurs. A dorsal midline laminectomy, including the caudal  
118 quarter of the lamina of L7 and a larger portion of the S1-S2 lamina, was performed  
119 with the aid of a surgical burr. The articular facet joints were left intact. The  
120 interarcuate ligament was resected and the epidural fat and cauda equina removed.  
121 Dorsal annulectomy was performed, creating a rectangular window in the central

122 dorsal annulus fibrosus, and nucleus pulposus material was removed with a Freer  
123 elevator from the central region of the disc (Fig 4A). The motion of the destabilized  
124 spine was then tested.

125

126 *Specimen preparation - Instrumented spine*

127 Using a dorsal approach (through the laminectomy), the tapered distraction bolt was  
128 driven into the center of the intervertebral space using a special applicator (Fig 4B),  
129 taking care to ensure that the top of the bolt came to rest flush with the ventral surface  
130 of the spinal canal (Fig 2). After drilling a hole with a 2mm drill, a 2.4-mm TTA  
131 screw was inserted from the floor of the vertebral canal (S1) through the central slots  
132 of the spacer into the caudal third of the L7 vertebra (Fig 2). For pedicle screw  
133 insertion in the L7 vertebra, the drill hole was made immediately subjacent to the  
134 mammillary process of the cranial articular process at the junction of the arch and the  
135 vertebral body. The screws were angled with the tip of the screw emerging in the mid-  
136 sagittal plane of the vertebral body (Figs 2A, 2B). For pedicle screw insertion in the  
137 sacrum, the entry point was cranial to the S1 neuroforamen and caudal to the caudal  
138 articular process of L7. The screw trajectory was directed into the alar wing of the  
139 sacrum, parallel to the sacroiliac joint but without encroaching on the joint (Figs 2A,  
140 2C). As the screws in L7 do not enter the pedicle from dorsal to ventral but enter the  
141 base of the pedicle where it joins the vertebral body, all drill holes were made with a  
142 3.2mm drill and an awl was not used. The *cis*-cortex was drilled and pedicle screws  
143 were inserted through the clamp, then screwed into the drill hole until their self-  
144 tapping tips just penetrated the *trans*-cortex. A washer was then placed on top of the  
145 pedicle screw head, the connecting rods were inserted (connecting the screws at L7

146 and S1) and then locked into the polyaxial clamp with a threaded nut screwed down  
147 onto the dumbbell head of the rod (Figs 2, 4C).

148

#### 149 *Motion Capture*

150 Relative angular displacements across the L6-L7 and L-S articulations were  
151 determined by measuring the relative movements of optical trackers with a dual-  
152 camera motion capture system (Polaris Vicra, Northern Digital Instruments, Waterloo,  
153 Ontario, Canada). For this purpose, three optical trackers (Polaris Vicra, Northern  
154 Digital Instruments, Waterloo, Ontario, Canada) were rigidly attached to L6, L7 and  
155 S1 using 3.2-mm Ellis pins. The dual-camera motion tracking system monitored the  
156 position of the motion trackers during the loading cycle. Each tracker consisted of  
157 four reflective marker balls arranged in a non-collinear fashion. For each applied  
158 moment, the motion of the vertebra was measured in 6 degrees of freedom (rotations  
159 and translations around the x-, y- and z- axes). Motions were described in relation to a  
160 coordinate system placed into the body.<sup>25</sup> Relative vertebral motions were calculated  
161 in terms of Euler angles by use of the angle sequence ZYX. In order to define the  
162 position of L6 and L7 in the testing volume and to define their zero position, a  
163 standardized series of anatomic landmarks on L6 and L7 was digitized. A total of four  
164 landmarks on each vertebra (L6 and L7) were marked with a drill hole and tissue  
165 marking dye (Fig 5) to ensure consistent identification. With the digitisation, Euler  
166 angle and translation of the specimen's motion trackers at L6, L7 and S1 were  
167 recorded simultaneously. S1 is considered fixed in the testing volume. The  
168 transformations gave the fixed coordinates of the four anatomical landmarks of L6  
169 and L7 relative to the tracker, making it possible to calculate relative positions of the  
170 vertebrae during testing. Before starting the first loading cycle, the positions of all of



171 the trackers was captured to document the neutral position of the spine. Subsequent  
172 changes in spinal angle and translation were then calculated. The same loading and  
173 data collection protocol was used for intact, destabilized and instrumented vertebral  
174 columns. Testing cycles for each spine were completed within four hours within a  
175 single day.

176

### 177 *Biomechanical Testing*

178 Mechanical testing was performed using a custom 4-point bending fixture.<sup>26</sup> The  
179 specimen was subjected to non-destructive compressive axial loads through a  
180 servohydraulic materials testing machine (Model 858, MTS Systems Corporation,  
181 Eden Prairie, MN) operating under load-control (Fig 6). Loads were applied from 0 to  
182 150N at the L6-L7 and L7-S1 junctions in the dorso-ventral (DV) direction to induce  
183 extension, ventro-dorsal (VD) direction to induce flexion, and the mediolateral (ML)  
184 direction to induce (left) lateral bending. Motions resulting from applying the load  
185 were measured and calculated by the motion tracking system and differentiated into  
186 the primary (intended) motions (e.g. extension with DV loading) and secondary  
187 (coupled) motions (e.g. axial rotation). After being placed in the testing machine, and  
188 after each change of position, the specimen was pre-loaded to minimize the effects of  
189 specimen viscoelasticity and to verify the optimal orientation of the tracking tools  
190 (Fig 6). L7 and L6 vertebrae were then digitized using four anatomic landmarks per  
191 vertebra (Fig 5). The specimen then underwent ramp loading in 25N increments to a  
192 maximum of 150N, with the load held for 5 seconds at each increment to allow time  
193 for motion tracking. The resulting motions of the FSU (functional spinal unit) were  
194 described in relation to the previously mentioned anatomical coordinate system.<sup>25</sup>

195

196 *Testing Steps and Instrumentation*

197 The specimens were tested sequentially in flexion, extension and left lateral bending  
198 as an intact spine, after decompressive surgery and after instrumentation with the new  
199 fixation system (Fig 7).

200

201 *Post-operative Evaluation*

202 Helical computed tomography scans (0.625 mm slice thickness) were obtained for  
203 every specimen to document the location and orientation of the spinal instrumentation  
204 used to stabilize the L-S junction. The screw trajectories were evaluated on transverse  
205 CT slices and analysed descriptively with a modified classification system reported in  
206 an earlier study (Fig 8).<sup>15</sup> Placement was considered optimal when the screw was  
207 positioned in the centre of the pedicle; acceptable placement was characterized by  
208 cortical encroachment of the medial pedicle wall; unacceptable placement was  
209 characterized by overt penetration of the medial pedicle wall and encroachment into  
210 the vertebral canal. The position of the stabilising wood screws in adjacent joints was  
211 also evaluated on CT.

212

213 *Data Analysis and Statistics*

214 Descriptive statistics of the data confirmed that they were normally distributed.  
215 Comparisons between intact, destabilised and stabilised groups were made using a  
216 one-way repeated measures analysis of variance (ANOVA) procedure with  
217 Bonferroni adjustment for post-hoc comparisons. The ANOVA model included  
218 factors related to the three treatment groups (intact, destabilised, instrumented) and  
219 the three loading protocols (i.e., extension, flexion, and left lateral bending).  
220 Statistical testing was performed using commercially available software (IBM SPSS

221 Statistics Version 20, International Business Machines Corp., Armonk, NY) and  
222 significance was set at  $p < 0.05$ . Each specimen served as its own control.

For Peer Review

## 223 RESULTS

224

### 225 *Diagnostic Imaging*

226 Screening radiographs from this series of dogs were unremarkable, with no evidence  
227 of spinal pathology. Radiographs of the potted prepared specimens showed that the  
228 wood screws were positioned appropriately across the L5-L6, S3-Cd1 and sacroiliac  
229 articulations, and no interference with the implants was detected on computed  
230 tomography post-operatively.

231

### 232 *Destabilisation with Laminectomy, Annulectomy and Discectomy*

233 The dimensions of the annulectomy and laminectomy defects in this study were based  
234 on those reported in previous studies.<sup>15,19,20</sup> The laminectomy defect had a mean ( $\pm$   
235 standard deviation, SD) width of  $12.8 \pm 0.9$  mm and length of  $31.1 \pm 2.9$  mm. The  
236 rectangular annulectomy defect measured  $4.8 \pm 0.9$  mm in length and  $9.8 \pm 0.7$  mm in  
237 width.

238

### 239 *Implants and Instrumentation*

240 The connecting rods used were 32 mm (4 of 16 specimens), 37 mm (9 of 16) or 42  
241 mm (3 of 16) in length and 4mm in diameter. The rods had to be bent to be able to  
242 place them over the facet joints in one specimen. The interbody bolts were generally  
243 positioned centrally within the intervertebral space (Fig 8D), with two bolts  
244 marginally deviated to the left and three spacers slightly tilted to the right in the  
245 sagittal plane. One bolt was seated incompletely and sat slightly above the ventral  
246 surface of the vertebral canal. All but one of the TTA screws were successfully placed  
247 through the slot in the bolt; in one specimen the drill bit broke but this was left in

248 place since it effectively served the same function as the screw in preventing rotation  
249 and back-out of the bolt. Screws implanted into L7 and S1 respectively had a length  
250 of 35mm (n=3 and n=13 respectively) and 40mm (n=13 and n=3 respectively). Post-  
251 operative CT scans revealed that all L7 and S1 pedicle screws engaged the *trans-*  
252 cortex. All L7 pedicle screws were placed through the pedicle and vertebral body and  
253 all S1 screws were placed in the alar wing. Accuracy of pedicle screw placement is  
254 shown in Fig 8 and Table 1.

255

### 256 *Kinematics of the Lumbosacral Spine*

257 Data collected at 25N were considered unreliable as they demonstrated significant  
258 early settling of the construct within the test frame, so only data from subsequent  
259 cycles were evaluated. Within each of the test constructs (intact, destabilised,  
260 instrumented) the patterns in angular displacement over load were consistent, so for  
261 reasons of clarity only the data from the highest load (150N) underwent statistical  
262 analysis.

263

264 *Primary motions:* Results for primary motion of L6-L7 and L7-S1 are summarized in  
265 Table 2 and graphically illustrated in Fig 9.

266

267 Range of motion in the L7-S1 joint in the intact and destabilised spine was higher  
268 than in the adjacent L6-L7 segment for flexion (**Fig 9A,  $p<0.05$** ) and extension (**Fig**  
269 **9B,  $p<0.05$** ) but showed similar values for lateral bending (**Fig 9C**). Destabilization  
270 resulted in increased extension at L7-S1 ( **$p=0.049$** ) but motions in flexion ( $p=0.20$ )  
271 and lateral bending ( $p=0.73$ ) were not increased. Destabilisation at L7-S1 was not  
272 associated with changes in motion at L6-L7. Following instrumentation, there was

273 near-complete elimination of primary motions at the instrumented L7-S1 level but no  
274 effect on motion at L6-L7, compared to the destabilised specimen. Motion at L7-S1  
275 following instrumentation was significantly lower than in the destabilized specimen in  
276 **flexion (Fig 9A, p=0.001), extension (Fig 9B, p=0.002) and lateral bending (Fig**  
277 **9C, p<0.001). Motion at the instrumented site was also lower than in the intact**  
278 **specimen for lateral bending (Fig 9C, p=0.015) but not flexion (Fig 9A, p=0.09)**  
279 **or extension (Fig 9B, p=0.09). Motion at L6-L7 was unaffected by**  
280 **instrumentation at L7-S1.**

281

282 *Secondary (coupled) motions:* Destabilization at L7-S1 was not associated with  
283 alterations in coupled motions as compared with intact specimens (Table 3).  
284 Instrumentation of L7-S1 resulted in statistically significant decreases in axial rotation  
285 during flexion, extension and lateral bending. Lateral bending during flexion and  
286 extension was also significantly reduced following instrumentation at L7-S1.

287

288 **DISCUSSION**

289 The key finding from this study was that instrumentation significantly reduced  
290 primary and coupled motion at L7-S1 following surgical decompression, lending  
291 support to our first hypothesis. Although there was a trend towards altered motion at  
292 the adjacent (L6-L7) level following destabilisation and instrumentation, these  
293 differences were not statistically significant, supporting our second hypothesis.

294

295 In the intact specimen, L7-S1 demonstrated high mobility in flexion and extension,  
296 and moderate mobility in lateral bending. The adjacent L6-L7 joint was significantly  
297 less mobile than L7-S1, confirming what has been shown in previous studies.<sup>27-29</sup> The  
298 L6-L7 segment showed a slightly higher mobility in lateral bending compared to  
299 extension and flexion, in contrary to a previous study.<sup>29</sup> These small differences (of a  
300 few degrees) between the current study and previous reports are likely explained by  
301 variations in test conditions. Coupled motion values in lateral bending and axial  
302 rotation in the present study might have shown higher values compared to a previous  
303 study<sup>29</sup> due to suboptimal technique of potting and/or digitization.

304

305 Decompressive surgery, with annulectomy and discectomy, **increased L7-S1 motion**  
306 **in extension but not in flexion or lateral bending**, as compared with the intact  
307 specimen. Results from human cadaveric studies have shown that annulus injury with  
308 discectomy alters the mechanical properties of the lumbar spinal unit, however  
309 without any significance<sup>30</sup> Similar observations were made in our study, in accordance  
310 with results of an earlier study in dogs<sup>19</sup>.

311

312 *Kinematics at L7-S1:* The significant decrease in primary motion of the L7-S1 joint  
313 following instrumentation was anticipated and is consistent with earlier work  
314 evaluating a more traditional pedicle screw-rod system.<sup>19</sup> However, the design of that  
315 earlier study was such that the authors could not discriminate between motions at L6-  
316 L7 versus L7-S1.<sup>19</sup> In our experiment, it was possible to evaluate motions at the two  
317 levels independently, providing greater insight into spinal kinematics after  
318 stabilisation. Our results are consistent with prior biomechanical studies in humans  
319 that have shown that pedicle screw fixation, alone or in combination with an  
320 intervertebral spacer, is a very effective method for stabilizing the lumbar spine.<sup>31,32</sup>

321

322 *Kinematics at L6-L7:* Instrumentation of the L7-S1 joint resulted in alterations in  
323 motion at the adjacent segment (L6-L7), but none of these changes was statistically  
324 significant. Although a previous paper has reported that immobilization of the canine  
325 lumbar spine with a pin and clamp construct increased segmental motion at the  
326 adjacent segment<sup>33</sup>, our results did not support this for the lumbosacral spine. Given  
327 the inherent variance in spinal motions in the intact and destabilised spines, and the  
328 potential confounding influence of differences in specimen size, it is perhaps not  
329 surprising that we were unable to identify a significant change at L6-L7. It is very  
330 possible that the limited sample size resulted in an increased risk of a type II (false  
331 negative) error. As a result, we remain cautious in interpreting the data relating to L6-  
332 L7 and would not exclude the possibility of adjacent level pathology (“domino  
333 lesion”) following rigid spinal fixation of the L-S junction.<sup>33</sup>

334

335 *Use of polyaxial clamps:* Although we describe the screws in this system as being  
336 pedicle screws, this is not correct in the purest sense. True pedicle screws are inserted



337 so that they run between the lateral and the medial walls of the pedicle.<sup>12,15,19,20</sup> In this  
338 system, the screws enter the pedicle but then deviate into the vertebral body.  
339 Cadaveric studies have shown that angulation of screws can increase screw pull-out  
340 strength in the lumbar spine.<sup>17</sup> Angling screws also makes it possible to achieve  
341 purchase in better quality bone and to avoid encroachment into critical anatomical  
342 structures such as the L6-L7 intervertebral space<sup>13</sup> and the sacro-iliac joint.<sup>34</sup> The  
343 novel implants used in this study and in clinical cases are made of titanium. Titanium  
344 spinal implants have been shown to have greater flexion stiffness in one-level  
345 instability compared to stainless steel constructs<sup>35</sup>, and people treated with titanium  
346 spinal implants were presented less often with late postoperative infections than those  
347 treated with stainless steel spinal implants.<sup>35</sup> Titanium alloy has found to be an  
348 appropriate material for dorsal spinal instrumentation rods because of its low weight,  
349 high biocompatibility and high tensile strength.<sup>36</sup>

350

351 *Distraction bolt:* Interbody cages have improved the fusion rates for spine surgery in  
352 humans<sup>37</sup> by allowing bone to grow from one vertebral endplate to the adjacent  
353 endplate via fenestrations in the cage. A threaded cage augmented with pedicle screw  
354 fixation is considered safe and effective for the treatment of lumbar and lumbosacral  
355 instability in humans, with a 96% fusion rate after 2 years.<sup>22</sup> The titanium distraction  
356 bolt used in the present study is tapered and cone-shaped, with fenestrations opposite  
357 each vertebral endplate and covered with hydroxyapatite. Hydroxyapatite (HA) has  
358 been shown to have excellent osteoconductive properties making it a useful scaffold  
359 where bone regeneration is needed.<sup>38</sup> This device has previously been used in  
360 conjunction with String-of-Pearl plates to achieve cervical distraction-stabilization in  
361 dogs.<sup>39</sup> The rationale for using it in combination with the screw-rod system was that

362 in addition to facilitating fusion, it will provide effective load sharing and decrease the  
363 risk of fatigue and subsequent implant failure.<sup>26</sup> To introduce the distraction bolt into  
364 the L7-S1 intervertebral space in-vivo, the cauda equina is retracted using a long,  
365 narrow instrument.<sup>40</sup>

366

367 *Limitations:* As with any cadaveric experiment, this study has a number of limitations  
368 that should be considered when interpreting the data. The potential impact of the  
369 relatively small sample size on statistical power has been mentioned. The absence of  
370 active muscle control means that the results from this study likely best reflect passive  
371 range of motion across L6-L7 and L7-S1. Every effort was made to eliminate motions  
372 outside of L6-L7 and L7-S1, but some residual instability may still have remained.  
373 We made a decision to limit testing to a maximum of 150N as this limit had been  
374 reported previously<sup>26</sup> and produced visible movements without any sign of  
375 impingement between the vertebrae. Testing was also limited to left lateral bending,  
376 although we felt that this was justifiable in terms of the symmetrical arrangement of  
377 the instrumentation around the spine. Finally, the new instrumentation was not tested  
378 against any other technique for lumbosacral instrumentation; comparative testing of  
379 this sort might have given valuable information about the performance of the different  
380 systems, especially with regard to discriminating the effects of instrumentation in  
381 general from those specific to a given implant system.

382

383 *Conclusion*

384 Application of a polyaxial screw-clamp fixation system in combination with an  
385 intervertebral distraction bolt has not been reported previously in the veterinary  
386 literature. The results from this cadaveric study demonstrate that the new implant

387 system restores stability to the lumbosacral junction following destabilisation, and  
388 supports application of this technique for the management of DLSS in dogs.<sup>40,41</sup>  
389 Clinical studies will be needed to determine the safety and long-term efficacy of the  
390 new fixation system, especially with regard to potential domino lesions at adjacent  
391 spinal levels.

392

393

For Peer Review

394 **REFERENCES**

395

396 1. Jeffery ND, Barker A, Harcourt-Brown T: What progress has been made in the  
397 understanding and treatment of degenerative lumbosacral stenosis in dogs during the  
398 past 30 years? *Vet J* 2014;201:9-14.

399

400 2. Ness MG: Degenerative lumbosacral stenosis in the dog: A review of 30 cases. *J*  
401 *Small Anim Pract* 1994;35:185-190.

402

403 3. Sharp NHJ, Wheeler SJ: Lumbosacral disease, in Sharp NHJ, Wheeler SJ (eds):  
404 *Small Animal Spinal Disorders: Diagnosis and Surgery*. Philadelphia, PA, Elsevier,  
405 2nd edition, 2005, pp 181-210.

406

407 4. Danielsson F, Sjöström L: Surgical treatment of degenerative lumbosacral stenosis  
408 in dogs. *Vet Surg* 1999;28:91-98.

409

410 5. Janssens LAA, Moens Y, Coppens P, et al: Lumbosacral degenerative stenosis in  
411 the dog: The results of dorsal decompression with dorsal anulectomy and nucleotomy.  
412 *Vet Comp Orthop Traumatol* 2000;13:97-103.

413

414 6. De Risio L, Sharp NJ, Olby NJ, et al: Predictors of outcome after dorsal  
415 decompressive laminectomy for degenerative lumbosacral stenosis in dogs: 69 cases  
416 (1987-1997). *J Am Vet Med Assoc* 2001;219:624-628.

417

- 418 7. Suwankong N, Meij BP, Voorhout G, et al: Review and retrospective analysis of  
419 degenerative lumbosacral stenosis in 156 dogs treated with dorsal laminectomy. *Vet*  
420 *Comp Orthop Traumatol* 2008;21:285-293.  
421
- 422 8. van Klaveren NJ, Suwankong N, De Boer S, et al: Force plate analysis before and  
423 after dorsal decompression for treatment of degenerative lumbosacral stenosis in  
424 dogs. *Vet Surg* 2005;34:450-456.  
425
- 426 9. Hanna FY: Lumbosacral osteochondrosis: radiological features and surgical  
427 management in 34 dogs. *J Small Anim Pract* 2001;42:272-278.  
428
- 429 10. Slocum B, Devine T: L7-S1 fixation-fusion for treatment of cauda equina  
430 compression in the dog. *J Am Vet Med Assoc* 1986;188:31-35.  
431
- 432 11. Auger J, Dupuis J, Quesnel A, et al: Surgical treatment of lumbosacral instability  
433 caused by discospondylitis in four dogs. *Vet Surg* 2000;29:70-80.  
434
- 435 12. Méheust P: Une nouvelle technique de stabilisation lombosacrée: l'arthrodese par  
436 visage pédiculaire, étude clinique de 5 cas. *Prat Méd Chir Anim Comp* 2000;35:201-  
437 207.  
438
- 439 13. Renwick AIC, Dennis R, Gemmill TJ: Treatment of lumbosacral discospondylitis  
440 by surgical stabilisation and application of a gentamicin-impregnated collagen  
441 sponge. *Vet Comp Orthop Traumatol* 2010;23:266-272.  
442

443 14. Hankin EJ, Jerran RM, Walker AM, et al: Transarticular facet screw stabilization  
444 and dorsal laminectomy in 26 dogs with degenerative lumbosacral stenosis with  
445 instability. *Vet Surg* 2012;41:611-619.

446

447 15. Smolders LA, Voorhout G, van de Ven R, et al: Pedicle screw-rod fixation of the  
448 canine lumbosacral junction. *Vet Surg* 2012;41:720-732.

449

450 16. Golini L, Kircher PR, Lewis FI, et al: Transarticular fixation with cortical screws  
451 combined with dorsal laminectomy and partial discectomy as surgical treatment of  
452 degenerative lumbosacral stenosis in 17 dogs: clinical and computed tomography  
453 follow-up. *Vet Surg* 2014;43:405-413.

454

455 17. Barber JW, Boden SD, Ganey T, et al: Biomechanical study of lumbar pedicle  
456 screws: does convergence affect axial pullout strength? *J Spinal Disord*  
457 1998;1998:215-220.

458

459 18. Watine S, Cabassu JP, Catheland S, et al: Computed tomography study of  
460 implantation corridors in canine vertebrae. *J Small Anim Pract* 2006;47:651-657.

461

462 19. Meij BP, Suwankong N, van der Veen AJ, et al: Biomechanical flexion-extension  
463 forces in normal canine lumbosacral cadaver specimens before and after dorsal  
464 laminectomy-discectomy and pedicle screw-rod fixation. *Vet Surg* 2007;36:742-751.

465

466 20. Tellegen AR, Willems N, Tryfonidou MA, et al: Pedicle screw-rod fixation: a  
467 feasible treatment for dogs with severe degenerative lumbosacral stenosis. *BMC Vet*  
468 *Res* 2015;11:299-311.

469

470 21. Wang M, Dalal S, Bagaria VB, et al: Changes in the lumbar foramen following  
471 anterior interbody fusion with tapered or cylindrical cages. *Spine J* 2007;7:563-569.

472

473 22. Zhang Y, Yang H, Wang J, et al: Two-year follow-up results after treatment of  
474 lumbar instability with titanium-coated fusion system. *Orthop Surg* 2009;1:94-100.

475

476 23. Choi KC, Ruy KS, Lee SH, et al: Biomechanical comparison of anterior lumbar  
477 interbody fusion: stand-alone interbody cage versus interbody cage with pedicle screw  
478 fixation – a finite element analysis. *BMC Musculoskelet Disord* 2013;14:200-228.

479

480 24. Boissiere L, Perrin G, Rigal J, et al: Lumbar-sacral fusion by a combined  
481 approach using interbody PEEK cage and posterior pedicle-screw fixation: clinical  
482 and radiological results from a prospective study. *Orthop Traumatol Surg Res*  
483 2013;99:945-951

484

485 25. White AA III, Panjabi M: Kinematics of the spine, in White AA III, Panjabi MM  
486 (eds): *Clinical biomechanics of the spine*. Philadelphia, PA, Lippincott, 1990, pp 85-  
487 125.

488

- 489 26. Hettlich BF, Allen MJ, Glucksman GS, et al: Effect of an intervertebral disc  
490 spacer on stiffness after monocortical screw/polymethylmethacrylate fixation in  
491 simulated and cadaveric canine cervical vertebral column. *Vet Surg* 2014;43:988-994.  
492
- 493 27. Bürger R, Lang J: Kinematic study of the lumbar and lumbosacral spine in the  
494 German Shepherd Dog. Part 2: own observations. *Schweiz Arch Tierheilk*  
495 1993;135:35-43.  
496
- 497 28. Hediger KU, Ferguson SJ, Gedet P, et al: Biomechanical analysis of torsion and  
498 shear forces in lumbar and lumbosacral spine segments of nonchondrodystrophic  
499 dogs. *Vet Surg* 2009;38:874-880.  
500
- 501 29. Benninger MI, Seiler GS, Robinson LE, et al: Three-dimensional motion pattern  
502 of the caudal lumbar and lumbosacral portions of the vertebral column of dogs. *Am J*  
503 *Vet Res* 2004;65:544-552.  
504
- 505 30. Goel VK, Nishiyama K, Weinstein JN, et al: Mechanical properties of lumbar  
506 spinal motion segments as affected by partial disc removal. *Spine* 1986;11:1008-1012.  
507
- 508 31. Boos B, Webb JK: Pedicle screw fixation in spinal disorders: a European view.  
509 *Eur Spine J* 1997;6:2-18.  
510
- 511 32. Vadapalli S, Robon M, Biyani A, et al: Effect of lumbar interbody cage geometry  
512 on construct stability: a cadaveric study. *Spine* 2006;31:2189-2194.  
513



- 514 33. Ha KY, Schendel MJ, Lewis JL, et al: Effect of immobilization and configuration  
515 on lumbar adjacent-segment biomechanics. *J Spinal Disord* 1993;6:99-105.  
516
- 517 34. Wheeler JL, Cross AR, Rapoff AJ: A comparison of the accuracy and safety of  
518 vertebral body pin placement using a fluoroscopically guided versus an open surgical  
519 approach: an in vitro study. *Vet Surg* 2002;31:468-474.  
520
- 521 35. Korovessis P, Baikousis A, Deligianni D, et al: Effectiveness of transfixation and  
522 length of instrumentation on titanium and stainless steel transpedicular spine implants.  
523 *J Spinal Disord* 2001;14:109-117.  
524
- 525 36. von Knoch M, Saxler G, Quint U: Titanium as an implant material for rods of  
526 transpedicular instrumentation of the lumbar spine. *Biomed Tech* 2004;49:132-136.  
527
- 528 37. Bagby GW: Arthrodesis by the distractive-compression method using a stainless  
529 steel implant. *Orthopedics* 1988;11:931-934.  
530
- 531 38. Olivares-Navarrete R, Gittens RA, Schneider JM, et al: Osteoblasts exhibit a more  
532 differentiated phenotype and increased bone morphogenetic protein production on  
533 titanium alloy substrates than on poly-ether-ether-ketone. *Spine J* 2012;12:265-272.  
534
- 535 39. Solano MA, Fitzpatrick N, Bertran J: Cervical distraction-stabilization using an  
536 intervertebral spacer screw and String-of Pearl (SOP<sup>TM</sup>) plates in 16 dogs with disc-  
537 associated wobbler syndrome. *Vet Surg* 2015;44:627-641.  
538

539 40. Fitzpatrick N: Degenerative lumbosacral stenosis: intervertebral spacer and screw-  
540 rod fixation system for distraction-fusion. *Proceedings of the 4<sup>th</sup> World Veterinary*  
541 *Orthopaedic Congress, 1-8 March 2014, Breckenridge, Colorado, pp. 137-138.*

542

543 41. Fitzpatrick N, Egan P, Murphy S, et al: Lumbosacral distraction-fusion using an  
544 intervertebral spacer and screw-rod fixation system for treatment of degenerative  
545 lumbosacral stenosis. *Proceedings of the 4<sup>th</sup> World Veterinary Orthopaedic Congress,*  
546 *1-8 March 2014, Breckenridge, Colorado p. 81.*

547

548

549

550

551 **FIGURE LEGENDS**

552

553 **Fig 1.** Photographs of the intervertebral distraction bolt (top: side view, bottom: view  
554 from on top) and the components of the pedicle-screw rod fixation system: clamp,  
555 3.5mm polyaxial screw, washer (bottom, notice the dipped inner circle and the  
556 indentation of the rim to accommodate the dumbbell-shaped rod), nut (top) and  
557 dumbbell-shaped connecting rod (from left to right).

558

559 **Fig 2.** Illustrations of the instrumented spine in the lateral (A) and transverse (B, C)  
560 planes, demonstrating the positioning and the trajectories of the pedicle screws,  
561 intervertebral distraction bolt, TTA screw, clamps and connecting rods.

562

563 **Fig 3.** Dorsoventral radiograph of canine specimen with the cranial (L5) and caudal  
564 (S3-Cd1) ends of the specimen potted in polyester resin and with the L-S junction  
565 centred between the potted ends. The L5-L6, S3-Cd1 and sacroiliac joints were  
566 immobilized with wood screws. For additional holding power, wood screws were  
567 inserted through the acetabulum into the ilial body, protruding 1cm within the potting  
568 medium. The cranial parts of the ilial wings have been removed. Drill holes, used as  
569 digitization points for the motion capture system, are visible bilaterally in the  
570 transverse processes of L6 and L7 and the base of the spinous processes of L6 and L7.

571

572 **Fig 4.** Photographs of the cadaveric specimen (A) in dorsal view after dorsal  
573 laminectomy and annulectomy, (B) in dorsolateral view with the intervertebral spacer  
574 connected to the applicator instrument while the spacer is screwed into the  
575 intervertebral space (note the Ellis pin for the motion tracker cranial to the applicator

576 and the spacer), (C) in dorsolaterocaudal view showing the polyaxial screws, clamps  
577 on both sides and a connecting rod applied on the right side.

578

579 **Fig 5.** Ventral (A) and right lateral (B) view of the stripped specimen (L6-S1) with  
580 digitization landmarks in two planes, marked with a drill hole and tissue marking dye.

581 The sagittal plane was defined by two digitization points cranial and caudal at the  
582 endplates in the ventral median plane (A, arrows) or cranial and caudal at the base of  
583 the spinous process (B, arrows). The transverse plane was defined by symmetric  
584 digitization points on the transverse processes (A, B –arrow heads).

585

586 **Fig 6.** Illustration of the biomechanical test set-up showing a representative  
587 lumbosacral specimen with ends potted in PVC cylinders. Retro-reflective optical  
588 trackers are rigidly attached to the vertebrae. The specimen is mounted on a 4-point  
589 bending jig and aligned with a servo-hydraulic materials testing machine.

590

591 **Fig 7.** Study design, illustrating the sequential testing as intact, destabilized and  
592 finally instrumented specimens.

593

594 **Fig 8.** Transverse computed tomography images of instrumented specimens. A, B:  
595 Images through the L7 vertebra demonstrating optimal (left screw in 8A, right screw  
596 in 8B), acceptable (right screw, 8A) and unacceptable (left screw, 8B) placement of  
597 pedicle screws. C: Image through S1 shows optimal (right screw) and acceptable  
598 placement (left screw) of pedicle screws and the TTA screw just ventral to the spinal  
599 canal. D: The transverse image through the L7-S1 intervertebral space depicts the

600 intervertebral distraction bolt positioned vertically within the intervertebral disc space,  
601 with its base lying flush with the ventral surface of the vertebral canal.

602

603 **Fig 9.** Bar graphs comparing the angular displacement of the L6-L7 (grey) and L7-S1  
604 (black) segments in intact, destabilized and instrumented spines under 150N of axial  
605 loading, resulting in flexion (A), extension (B) and left lateral bending (C) as primary  
606 motion. **Lines indicate significant differences (and associated p-values) between**  
607 **treatments or levels, as appropriate.**

608



Fig 1. Photographs of the intervertebral distraction bolt (top: side view, bottom: view from on top) and the components of the pedicle-screw rod fixation system: clamp, 3.5mm polyaxial screw, washer (bottom, notice the dipped inner circle and the indentation of the rim to accommodate the dumbbell-shaped rod), nut (top) and dumbbell-shaped connecting rod (from left to right).

195x110mm (300 x 300 DPI)

Review

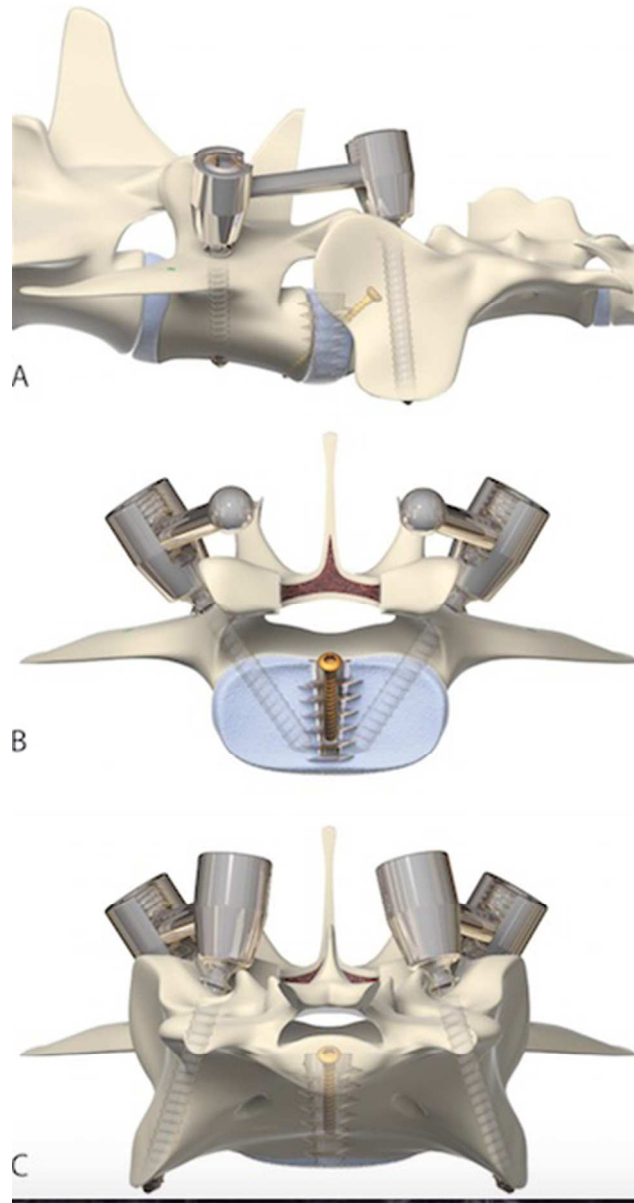


Fig 2. Illustrations of the instrumented spine in the lateral (A) and transverse (B, C) planes, demonstrating the positioning and the trajectories of the pedicle screws, intervertebral distraction bolt, TTA screw, clamps and connecting rods.

80x151mm (300 x 300 DPI)

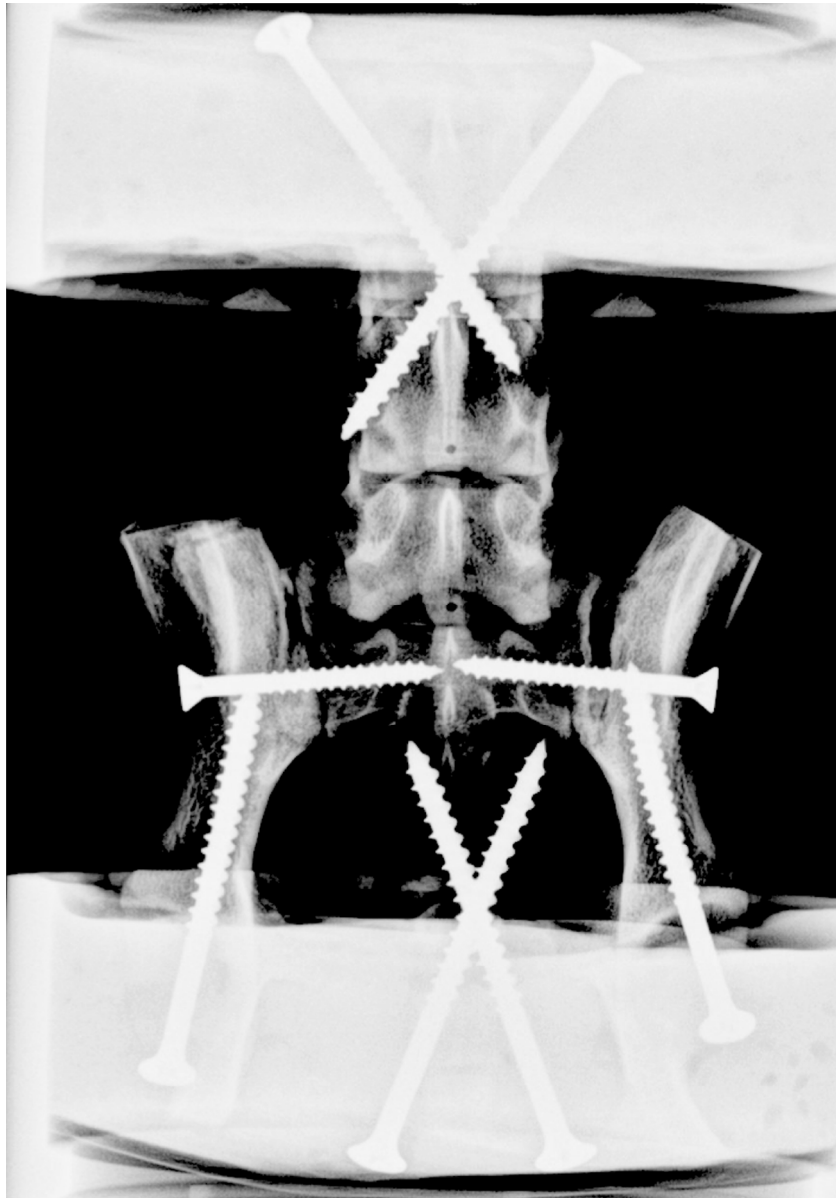


Fig 3. Dorsoventral radiograph of canine specimen with the cranial (L5) and caudal (S3-Cd1) ends of the specimen potted in polyester resin and with the L-S junction centred between the potted ends. The L5-L6, S3-Cd1 and sacroiliac joints were immobilized with wood screws. For additional holding power, wood screws were inserted through the acetabulum into the ilial body, protruding 1cm within the potting medium. The cranial parts of the ilial wings have been removed. Drill holes, used as digitization points for the motion capture system, are visible bilaterally in the transverse processes of L6 and L7 and the base of the spinous processes of L6 and L7.

91x130mm (300 x 300 DPI)



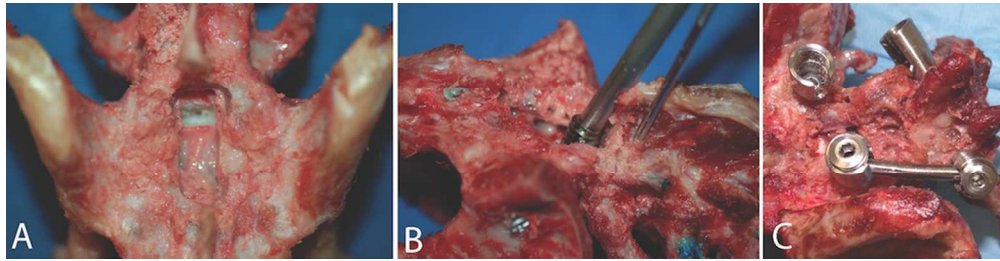


Fig 4. Photographs of the cadaveric specimen (A) in dorsal view after dorsal laminectomy and annulectomy, (B) in dorsolateral view with the intervertebral spacer connected to the applicator instrument while the spacer is screwed into the intervertebral space (note the Ellis pin for the motion tracker cranial to the applicator and the spacer), (C) in dorsolaterocaudal view showing the polyaxial screws, clamps on both sides and a connecting rod applied on the right side.

150x38mm (300 x 300 DPI)

Peer Review

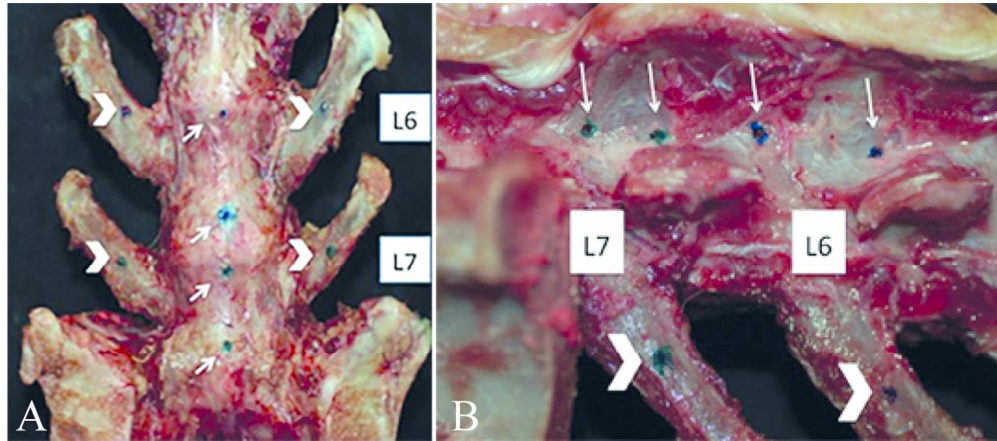


Fig 5. Ventral (A) and right lateral (B) view of the stripped specimen (L6-S1) with digitization landmarks in two planes, marked with a drill hole and tissue marking dye. The sagittal plane was defined by two digitization points cranial and caudal at the endplates in the ventral median plane (A, arrows) or cranial and caudal at the base of the spinous process (B, arrows). The transverse plane was defined by symmetric digitization points on the transverse processes (A, B -arrow heads).

144x62mm (300 x 300 DPI)

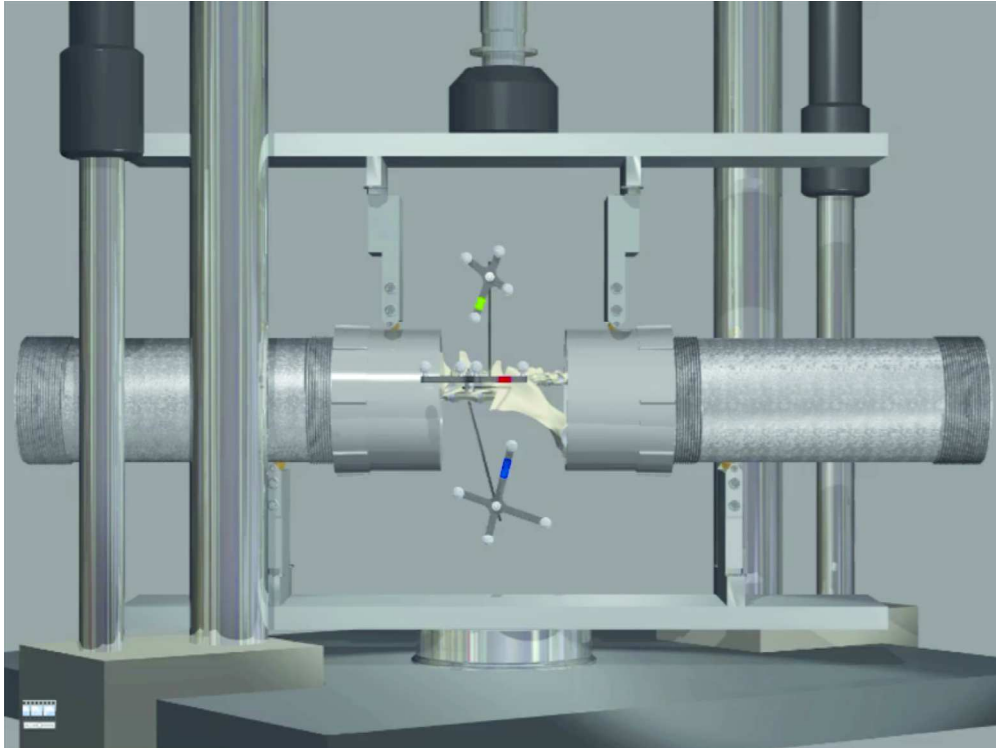


Fig 6. Illustration of the biomechanical test set-up showing a representative lumbar specimen with ends potted in PVC cylinders. Retro-reflective optical trackers are rigidly attached to the vertebrae. The specimen is mounted on a 4-point bending jig and aligned with a servo-hydraulic materials testing machine.

146x109mm (300 x 300 DPI)

view

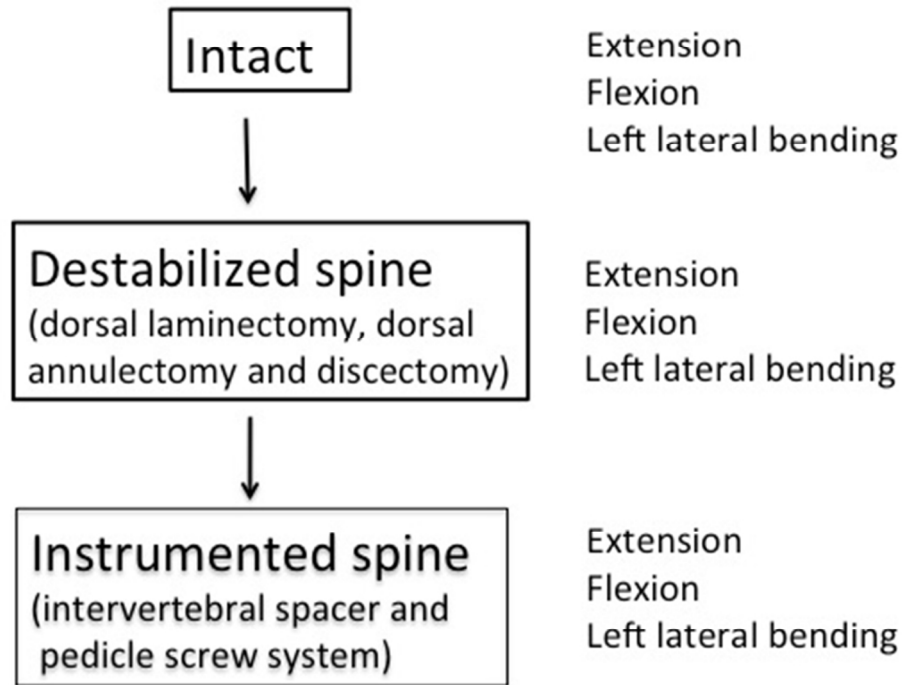


Fig 7. Study design, illustrating the sequential testing as intact, destabilized and finally instrumented specimens.

119x92mm (300 x 300 DPI)

view

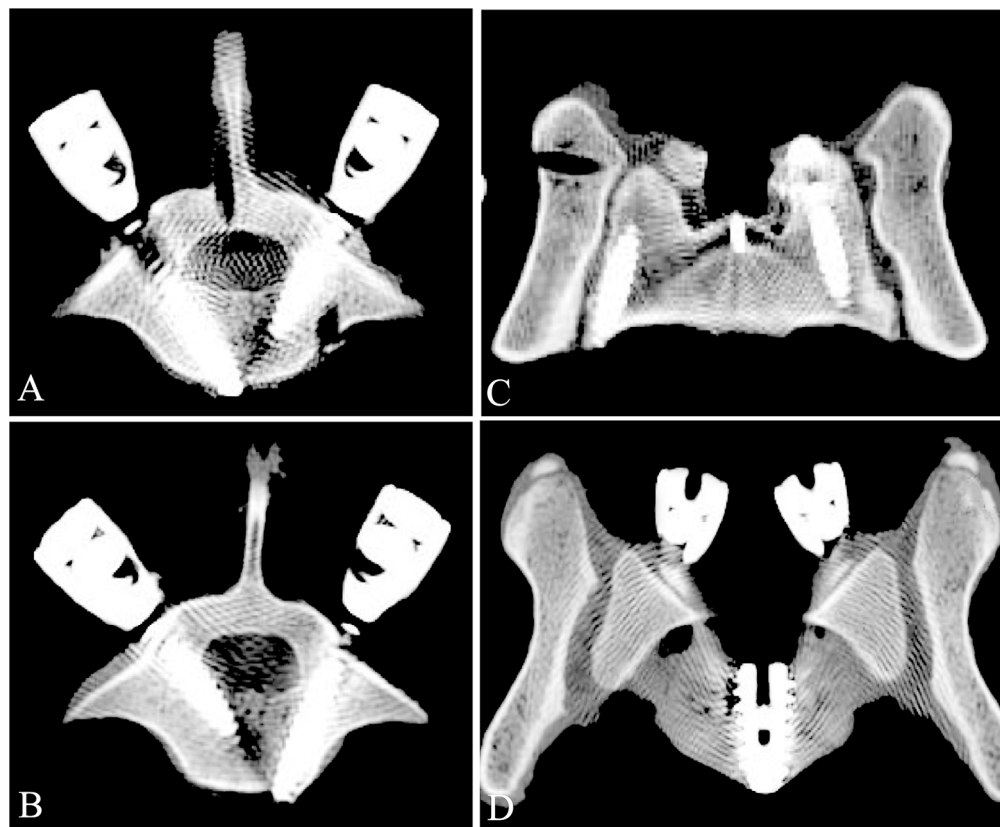


Fig 8. Transverse computed tomography images of instrumented specimens. A, B: Images through the L7 vertebra demonstrating optimal (left screw in 8A, right screw in 8B), acceptable (right screw, 8A) and unacceptable (left screw, 8B) placement of pedicle screws. C: Image through S1 shows optimal (right screw) and acceptable placement (left screw) of pedicle screws and the TTA screw just ventral to the spinal canal. D: The transverse image through the L7-S1 intervertebral space depicts the intervertebral distraction bolt positioned vertically within the intervertebral disc space, with its base lying flush with the ventral surface of the vertebral canal.

168x138mm (300 x 300 DPI)

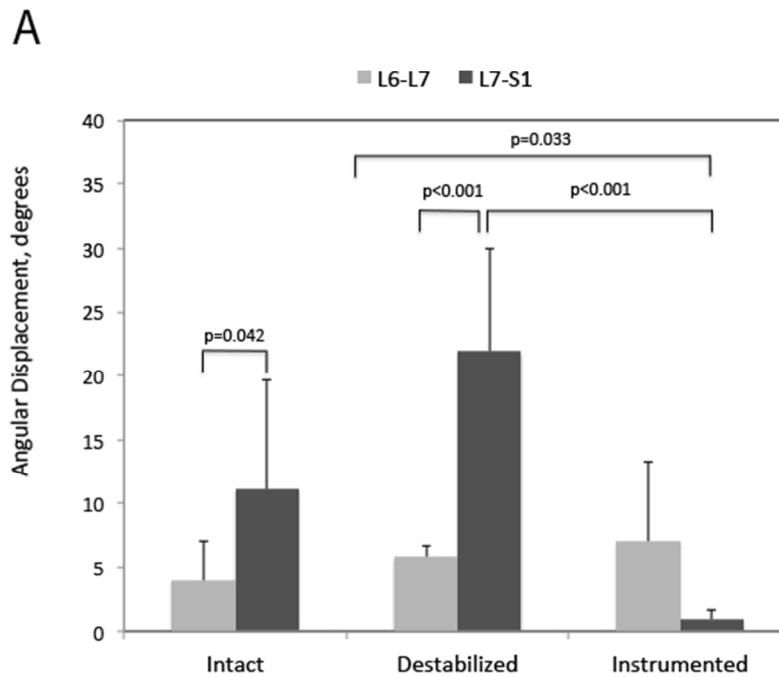


Fig 9. Bar graphs comparing the angular displacement of the L6-L7 (grey) and L7-S1 (black) segments in intact, destabilized and instrumented spines under 150N of axial loading, resulting in flexion (A), extension (B) and left lateral bending (C) as primary motion. Lines indicate significant differences (and associated p-values) between treatments or levels, as appropriate.

229x184mm (72 x 72 DPI)

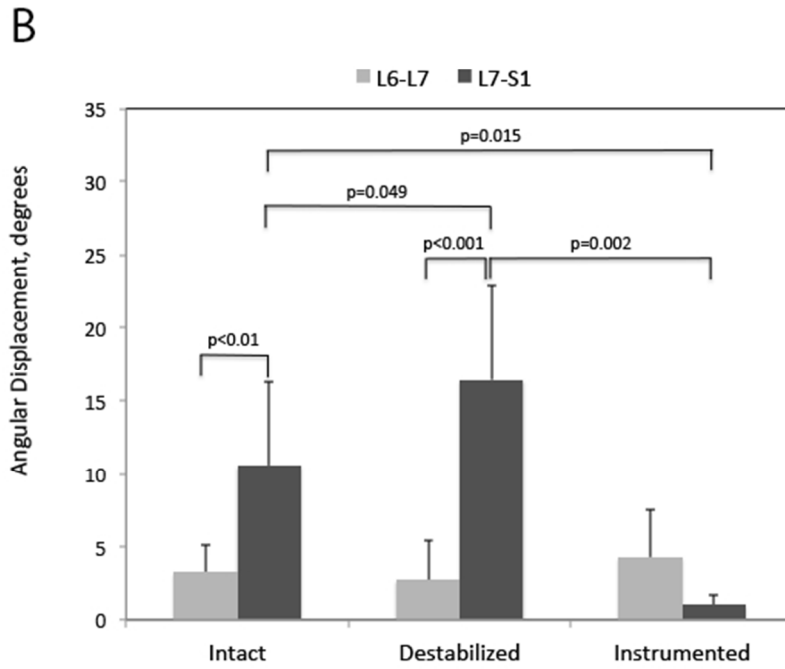


Fig 9. Bar graphs comparing the angular displacement of the L6-L7 (grey) and L7-S1 (black) segments in intact, destabilized and instrumented spines under 150N of axial loading, resulting in flexion (A), extension (B) and left lateral bending (C) as primary motion. Lines indicate significant differences (and associated p-values) between treatments or levels, as appropriate.

229x184mm (72 x 72 DPI)

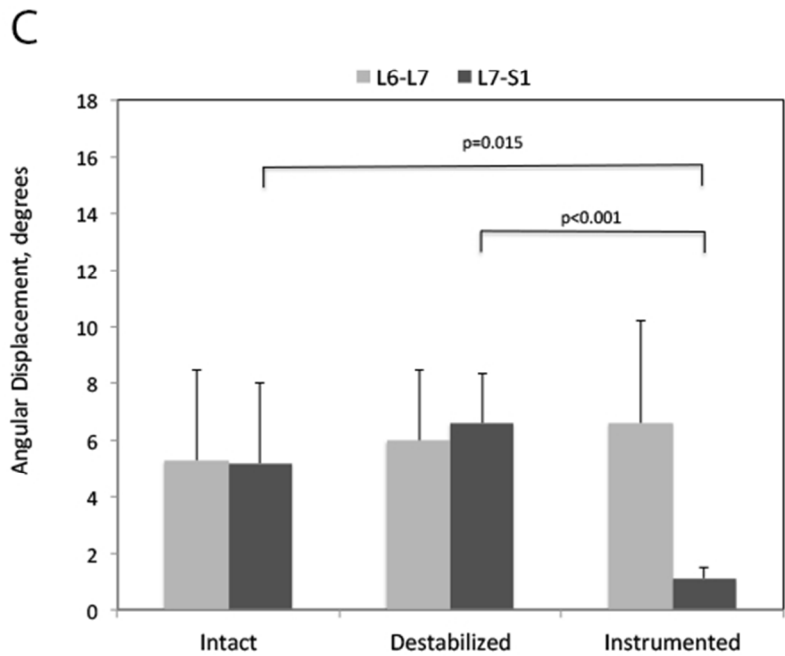


Fig 9. Bar graphs comparing the angular displacement of the L6-L7 (grey) and L7-S1 (black) segments in intact, destabilized and instrumented spines under 150N of axial loading, resulting in flexion (A), extension (B) and left lateral bending (C) as primary motion. Lines indicate significant differences (and associated p-values) between treatments or levels, as appropriate.

229x184mm (72 x 72 DPI)



**Table 1.** Number of pedicle screws (L7 and S1) with optimal, acceptable or unacceptable placement, evaluated post-operatively on computed tomography using a modified classification system.

Placement	L7 screws	S1 screws
Optimal	9/16	15/16
Acceptable	5/16	1/16
Unacceptable	2/16	0/16

**Table 2.** Primary motions at L6-7 and L7-S1 in the cadaveric canine lumbosacral spine in the intact state, following destabilization (dorsal laminectomy and partial discectomy at L7-S1) and after instrumentation at L7-S1 segment with the novel fixation system. Primary motions, in degrees, are reported as mean  $\pm$  SD (range) for flexion, extension and lateral bending tests performed under 150N loading.

		L6-L7			L7-S1		
	Primary Motion	Intact	Destabilized	Instrumented	Intact	Destabilized	Instrumented
VD	Flexion	3.9 $\pm$ 3.2	5.8 $\pm$ 0.9	7.0 $\pm$ 6.3	11.1 $\pm$ 8.5 <sup>c</sup>	20.0 $\pm$ 9.3 <sup>c</sup>	0.9 $\pm$ 0.7 <sup>ab</sup>
DV	Extension	3.2 $\pm$ 1.9	2.7 $\pm$ 2.7	4.3 $\pm$ 3.2	9.8 $\pm$ 5.7 <sup>bc</sup>	16.4 $\pm$ 6.5 <sup>ac</sup>	1.0 $\pm$ 0.7 <sup>ab</sup>
ML	Lateral bending	5.3 $\pm$ 3.2	6.0 $\pm$ 2.5	6.6 $\pm$ 3.6	5.2 $\pm$ 2.8 <sup>c</sup>	6.6 $\pm$ 1.7 <sup>c</sup>	1.1 $\pm$ 0.4 <sup>ab</sup>

Superscript letters denote significant differences ( $p < 0.05$ ) from intact<sup>a</sup>, destabilized<sup>b</sup> or instrumented<sup>c</sup> specimens.

**Table 3.** Coupled motions (axial rotation or lateral bending) at the L7-S1 segment in the intact spine, following destabilization (dorsal laminectomy-partial discectomy at L7-S1) and after instrumentation with the novel fixation system. Data, in degrees, are reported as mean  $\pm$  SD for flexion, extension and lateral bending tests performed under 150N loading.

Loading Direction	Secondary Motions	Intact	Destabilized	Instrumented
Flexion	Axial rotation	9.4 $\pm$ 8.3	11.5 $\pm$ 8.2 <sup>c</sup>	0.9 $\pm$ 0.7 <sup>b</sup>
	Lateral bending	10.6 $\pm$ 11.1	4.2 $\pm$ 6.8	0.7 $\pm$ 0.5
Extension	Axial rotation	12.5 $\pm$ 8.8 <sup>c</sup>	10.2 $\pm$ 7.0 <sup>c</sup>	0.5 $\pm$ 0.4 <sup>ab</sup>
	Lateral bending	12.4 $\pm$ 5.7 <sup>c</sup>	8.5 $\pm$ 4.7 <sup>c</sup>	0.6 $\pm$ 0.6 <sup>ab</sup>
Lateral bending	Axial rotation	4.7 $\pm$ 2.5 <sup>c</sup>	4.4 $\pm$ 2.9 <sup>c</sup>	0.4 $\pm$ 0.3 <sup>ab</sup>

Superscript letters denote significant differences ( $p < 0.05$ ) from intact<sup>a</sup>, destabilized<sup>b</sup> or instrumented<sup>c</sup> specimens.